JJMIE

Volume 3, Number 3, September 2009
ISSN 1995-6665
Pages 206 - 215

Jordan Journal of Mechanical and Industrial Engineering

The Effect of Fatigue on Crack Propagation in Flat Plates under Buckling Bending and Shear

Fathi A. Al-Shamma*

Mechanical Engineering Department, College of Engineering, University of Baghdad, Baghdad, Iraq

Abstract

Many works have been carried out to determine expressions for critical loads of crack propagation in flat plates under elementary load cases of shear, compression, bending and combination of theme. In this new solution, the analytical work must take into consideration the effect of fluctuating the buckling load for panels under various types of bending and shear loading. The effect of combined buckling shear and bending stresses on the crack propagation has been considered in this research. The analytical solution is based on a combination of maximum strain under mixed mode, Paris and Sih equation with Forman et al. equation. Different boundary conditions must be included in the flat plates, and new stress intensity factors for combined modes I and II have been developed for the crack growth. Also the results show the effect of crack length on the stress distribution and the direction of crack propagation.

Keywords: Buckling Bending; Shear; Crack Propagation Fatigue; Stress Intensity Factors (KI, KII).

1. Introduction

In structures formed from thin sheets of material, there is an additional possible mode of instability known as local buckling. When a thin rectangular sheet is subjected to loads which can potentially cause failure by buckling, these loads comprise combinations of compression, shear and bending forces. Generic to all of these cases is the existence of stress gradients across the shells.

Previous researchers have carried out work mainly based on the use of energy methods such as the Raleigh – Ritz method [1], to determine theoretical buckling loads for panels under pure shear, compression, and combinations of these. These cases are summarized in design guides such as those by young [2], Timoshenko and Gere [3] and Bruhn [4]. However, this work is fairly limited in that it assumes a constant stress distribution and only very simple boundary conditions such as four edges simply supported, or four edges clamped have been considered.

Featherstone [5] outlines a programmed work that has been under taken to compare collapse loads predicted by theoretical, experimental, and finite element. Analysis predicted collapse loads for the case of a flat rectangular plate under combined shear and bending.

A great deal of research has been devoted to a study of the mechanism of fatigue, and yet there is still not a complete understanding of the phenomenon and the effect of fatigue loading on the crack propagation under complex stress of boundary conditions. Knowledge of the initiation site and subsequent growth path of a fatigue crack greatly assists in determining the mode of failure and severity of its consequences. In addition, knowledge of the stress intensity factors at the various stages of growth is used to ascertain the service life of such components. (Nurse and patter son) [6]. D.R.Tadjiev et al. [7] studied the fatigue crack growth prediction under random loading in specimens of high strength aluminum alloy using modified root mean square (RMS) model for each specimen to determine the max. And min stresses under constant amplitude loading, R.Doglione and M. Bartolone [8] studied the fatigue crack propagation in a 2195-T8 alloy plate. They showed that fatigue resistance of this alloy is comparable to that of the classical competitor alloys and high lights stress ratio effects on the behavior at the threshold which causes the stress intensity range (Δkth) decrease as R increases . Yongming Liu et al. [9] developed a new mixed mode threshold stress intensity factor using a critical plane based multiaxial fatigue theory and the Kitagawa diagram. The proposed method is a nominal approach since the fatigue damage is evaluated using remote stresses acting on the cracked component rather than stresses near the crack tip.

An alternative method for determining the fluctuating of buckling load and its effect on the crack propagation in thin shells under complex load cases by using combined methods of max strain and max stress was done in this research. This has the advantage of allowing more difficult boundary conditions to be modeled, and loads to be applied as they exist in situ, thereby recreating varying stresses fields within the panel. This paper calculates the buckling loads for plates of four aspect ratios with different crack of lengths.

* Corresponding author. Fathi_alshamma@yahoo.com.

2. Theory

2.1. Fracture Mechanics for Fatigue

Fracture mechanics can only be applicable to fatigue after the crack initiation phase to enable crack growth to be predicted. As stated earlier fatigue failure is generally considered to be a three – stage process:

2.1.1. Stage I The Initiation of a Crack

There is some doubt as to where this occurs, and the processes of nucleation and stage 1 growth are not fully understood.

Using electron microscopically techniques for observing extrusions and intrusions from well defined slip bands [10] and have been proposed a theory of cross slip or slip on alternate slip planes and initially the cracks will be formed [11]. These cracks are likely to be aligned with the direction of maximum shear within the component i.e. at 45 ̊to the maximum principle stress. Hence nominally, the position of maximum tangential stress has been used; and assumes that surface flaws are homogeneously distributed and will from the site of a crack initiation. This method has been used taking into consideration the effect of friction on the crack propagation [21].

2.1.2. Stage II Crack Propagation

After initiation, crack propagation occurs as stage II growth according to [10]. Description of fatigue crack growth which attempts to include stage 1 and 2 growth in the determination of crack path would necessitate knowledge of the transition between stage 1 and 2 growth. Stage 1 growth occurs immediately which often grow with a strong shear component. Most cracks move to stage 2 growths with increasing crack length, which is characterized by macroscopic effects with crack is characterized by macroscopic effects with crack growth dominated by mode I displacements.

2.1.3. Stage III Crack Acceleration

When the crack has grown so that the critical stress intensity factor KIc is approached, the crack accelerates more rapidly with non linear relation until KIc is exceeded, and a final catastrophic failure occurs. This is related to the amplitude of the stress intensity factor Δk during the cycle which increases in this stage.

3. Crack Growth Laws

For many materials stage II, growth is described by the Paris-Erdogan law which is:-

$$\frac{da}{dN} = c(\Delta k)^m$$

Where c and m material coefficients (m lies between 2 and 7)

This simple relationship can be used to predict life time of component if the stress amplitude is constant.

However, when stress amplitude varies, then the growth rate may depart markedly from the simple relation, and then Forman equation could be used, which also describe stage III.

The propagation of the crack in stage 2 has been predicted in this study assuming brittle failure. It has been shown that stress and strain methods are more reliable than those based on strain energy criteria. This is especially true when there is a mixed mode crack [12].

Added to this, the stress and strain based methods , found in ASTM standard E647 – 939 [20] have more readily understood physical basis, which essentially states that failure will occur in the direction perpendicular to the largest stress or strain.

In this study, the method used for determining the direction of crack growth by using maximum principle strain which comes from mixing two modes, I and II, by applying fluctuating buckling stress. The method adopted was based also on the maximum circumferential stress and its direction with the crack propagation. The values of the ratio KII to KI was predicted and was improved by satisfying these values, mathematical approach in [13].

From these ratios of KII / KI, we can find ΔK, and then using them to find the crack growth rate in the expression of formans under mixed bending and torsion stresses.

4. Theoretical Analysis

For a plate with simply supported edges and the crack propagate by two modes I and II because the buckling of rectangular plates with mixed boundary conditions under combination of bending and shear as shown in fig 1(a-b) could be Equivalent to state two conditions**:**

4.1. Shear

The problem of shear buckling for long strips and plates has been studied by many works.Some workers [14] used Donnells equations to investigate the buckling of long plates under shear with both simply supported and clamped edges for the whole curvature range. This work has shown that the critical stress of a panel in shear buckling can be written as:

$$\tau_{cr} = \frac{Ks \cdot \pi^2 \cdot E}{12\,(1 - \mu^2)} \left(\frac{t}{b}\right)^2$$

Where

a= length of longer side of plate

E=young's modulus

b=length of shorter side of plate

Ks=shear buckling stress parameter

t= thickness of plate

μ=Poisson's ratio.

Ks varies a according to the boundary condition and aspect ratio. It has been looked at the case of a rectangular plate with one edge clamped using a Fourier series to represent the deflection of the plate in the energy equations [15]. Values of Ks are shown in table (1).

4.2. Bending

To solve the problem of a rectangular plate with simply supported edges, it has been used the principle of conservation of energy and a deflection in the form of a double trigonometric function [3]. For pure bending, the critical load can be calculated by the formula:

$$\sigma_{cr} = \frac{Kb \cdot \pi^2 \cdot E}{12\,(1 - \mu\,2)} \left(\frac{t}{b}\right)^2$$

Where
Kb= bending buckling stress parameter.
Kb varies according to the boundary condition and aspect ratio values of Kb are shown in table (2)

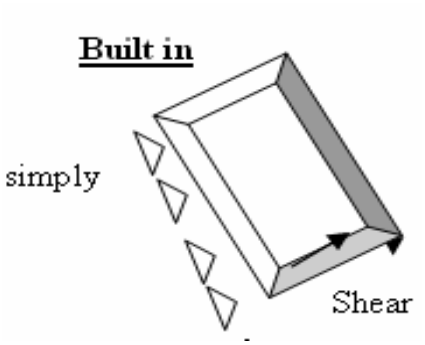

(a)

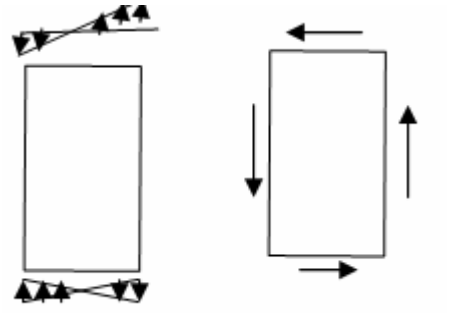

(b)

Figure 1(a),(b). Applied stress distribution on the edges of the plate.

Table 1. values of Ks for rectangular plate with one edge clamped

a/b	2.5	2	1.5	1.25	1.11	1.0
Ks	7.96	6.72	7.59	8.57	9.66	10.98

Table 2 .values of Kb for rectangular plate with simply supported

a/b	0.6	0.75	0.8	0.9	1	1.5	2.	2.5
Kb	2.41	2.42	2.44	2.56	2.56	2.41	2.39	2.38

5. Equations for the Relation of Fatigue Buckling and Crack Propagation:

The relation between fatigue buckling and crack propagation can be divided to three groups:
1) For the displacement of the crack
Propagation in the x-direction:

$$u = u_{modeI} + U_{modeII} = u_I + u_{II} \quad (1)$$

$$\therefore \frac{\partial u}{\partial x} = \frac{\partial u_I}{\partial x} + \frac{\partial u_{II}}{\partial x}$$

$$\therefore \in_x = \in_{xI} + \in_{xII} \quad (2)$$

For plane stress, Hooke's law applied as:

$$E \in_x = \sigma_x - \nu(\sigma_y) \quad (3)$$

for mode I :

$$\left.\begin{aligned} \sigma_x &= \frac{K_I}{\sqrt{2\pi r}} Cos\ \frac{\theta}{2}(1 - Sin\ \frac{\theta}{2} Sin\ \frac{3\theta}{2}) \\ \sigma_y &= \frac{K_I}{\sqrt{2\pi r}} Cos\ \frac{\theta}{2}(1 + Sin\ \frac{\theta}{2} Sin\ \frac{3\theta}{2}) \\ \tau_{xy} &= \frac{KI}{\sqrt{2\pi r}} Sin\ \frac{\theta}{2} Cos\ \frac{\theta}{2} Cos\ \frac{3\theta}{2} \end{aligned}\right\} \quad (4)$$

substitute eq(4) in (3):

$$E\in_{xI} = \frac{K_I}{\sqrt{2\pi r}} Cos\frac{\theta}{2}(1 - Sin\frac{\theta}{2} Sin\frac{3\theta}{2}) - \nu(\frac{K_I}{\sqrt{2\pi r}} Cos\frac{\theta}{2}(1 + \sin\frac{\theta}{2} Sin\frac{3\theta}{2}) \quad (5)$$

For mode II :

$$\left.\begin{aligned} \sigma_x &= \frac{-K_{II}}{\sqrt{2\pi r}} Sin\ \frac{\theta}{2}(2 + \text{Cos}\ \frac{\theta}{2} Cos\ \frac{3\theta}{2}) \\ \sigma_y &= \frac{K_{II}}{\sqrt{2\pi r}} Sin\ \frac{\theta}{2}(Cos\ \frac{\theta}{2} Cos\ \frac{3\theta}{2}) \\ \tau_{xy} &= \frac{K_{II}}{\sqrt{2\pi r}} Cos\ \frac{\theta}{2}(1 - \text{Sin}\ \frac{\theta}{2} Sin\ \frac{3\theta}{2}) \end{aligned}\right\} \quad (6)$$

Substitute eq(6) in eq(4) :-

$$E\in_{xII} = \frac{-K_{II}}{\sqrt{2\pi r}} \sin\frac{\theta}{2}(2 + \cos\frac{\theta}{2}\cos\frac{3\theta}{2}) - \nu\frac{K_{II}}{\sqrt{2\pi r}} \sin\frac{\theta}{2}(\cos\frac{\theta}{2}\cos\frac{3\theta}{2}) \quad (7)$$

From eq 2 we could obtain:

$$\in_x = \frac{1}{E}(\frac{KI}{\sqrt{2\pi r}} Cos\frac{\theta}{2}(1 - \text{Sin}\frac{\theta}{2}\text{Sin}\frac{3\theta}{2}) - \nu(\frac{\text{KI}}{\sqrt{2\pi r}} Cos\frac{\theta}{2}(1 + Sin\frac{\theta}{2} Sin\frac{3\theta}{2})))$$
$$+ \frac{1}{E}(\frac{-\text{K}_{\text{II}}}{\sqrt{2\pi r}} Sin\frac{\Theta}{2}(2 + Cos\frac{\theta}{2} Cos\frac{3\theta}{2}) - \nu(\frac{\text{KII}}{\sqrt{2\pi r}} Sin\frac{\theta}{2}(Cos\frac{\theta}{2} Cos\frac{3\theta}{2}))). \quad (8)$$

For Combined mode I and II of the

$$\in_Y = \frac{1}{E}(\frac{K_I}{\sqrt{2\pi r}} Cos\frac{\theta}{2}(1 - \text{Sin}\frac{\theta}{2}\text{Sin}\frac{3\theta}{2}) - \nu(\frac{\text{K}_{\text{II}}}{\sqrt{2\pi r}} Cos\frac{\theta}{2}(1 + Sin\frac{\theta}{2} Sin\frac{3\theta}{2}))) \quad (9)$$

$$\gamma_{xy} = \frac{2(1+\nu)}{E}\tau_{xy} = \frac{2(1+\nu)}{E}(\frac{Ki}{\sqrt{2\pi r}} \text{Sin}\frac{\theta}{2} Cos\frac{\theta}{2} Cos\frac{3\theta}{2} + \frac{K_{II}}{\sqrt{2\pi r}} Cos\frac{\theta}{2}(1 - \text{Sin}\frac{\theta}{2}\text{Sin}\frac{3\theta}{2})] \quad (10)$$

propagation of the crack it can be seen that mode II change the crack displacement in the x direction only, that is mean:
$V=V_I$ where V is the displacement in the y direction
So that we could find in polar coordinate:

$$\in_\theta = \frac{1}{2}(\in_x + \in_y) + \frac{1}{2}(\in_x - \in_y)\cos 2\theta + \frac{1}{2}\gamma_{xy}\sin 2\theta \quad (11)$$

By substituting eq 8, 9 and 10 in equation 11

$$\nu(\frac{K_{\text{II}}}{\sqrt{2\pi r}} Sin\frac{\theta}{2}(Cos\frac{\theta}{2} Cos\frac{3\theta}{2}))) + \frac{1}{2E}(\frac{K_I}{\sqrt{2\pi r}} Cos\frac{\theta}{2}[1\_\text{Sin}\frac{\theta}{2} Sin\frac{3\theta}{2} - 1 - \text{Sin}\frac{\theta}{2} Sin\frac{3\theta}{2}]$$
$$- \nu\frac{\text{K}_{\text{I}}}{\sqrt{2\pi r}} Cos\frac{\theta}{2}[1 + Sin\frac{\theta}{2} Sin\frac{3\theta}{2} - 1 + \text{Sin}\frac{\theta}{2} Sin\frac{3\theta}{2}]) + \frac{1}{2E}(-\frac{\text{K}_{\text{II}}}{\sqrt{2\pi r}} Sin\frac{\theta}{2}(2 +$$
$$Cos\frac{\theta}{2} Cos\frac{3\theta}{2}) - \nu(\frac{\text{K}_{\text{II}}}{\sqrt{2\pi r}} Sin\frac{\theta}{2}(Cos\frac{\theta}{2} Cos\frac{3\theta}{2}))) Cos2\theta + \frac{1+\nu}{E} Sin2\theta[$$

$$\in_\theta = \frac{1}{2E}(\frac{K_I}{\sqrt{2\pi r}} Cos\frac{\theta}{2}[1 - \text{Sin}\frac{\theta}{2}\text{Sin}\frac{3\theta}{2}] - \nu(\frac{\text{K}_{\text{I}}}{\sqrt{2\pi r}}(Cos\frac{\theta}{2}[1 +$$
$$\text{Sin}\frac{\theta}{2}\text{Sin}\frac{3\theta}{2} + 1 - \text{Sin}\frac{\theta}{2}\text{sin}\frac{3\theta}{2}])) + \frac{1}{2E}(\frac{K_{II}}{\sqrt{2\pi r}} \sin\frac{\theta}{2}(2 + \cos\frac{\theta}{2}\cos\frac{3\theta}{2}) -$$

$$\frac{k_I}{\sqrt{2\pi r}} Sin\frac{\theta}{2} Cos\frac{\theta}{2} Cos\frac{3\theta}{2} + \frac{k_{II}}{\sqrt{2\pi r}} Cos\frac{\theta}{2}\left(1 - Sin\frac{\theta}{2} Sin\frac{3\theta}{2}\right)$$

$$\therefore \varepsilon\theta = \frac{1}{2E}\left(\frac{2k_I}{\sqrt{2\pi r}} Cos\frac{\theta}{2} - \frac{\upsilon 2k_I}{\sqrt{2\pi r}} Cos\frac{\theta}{2}\right) + \frac{1}{2E}\left(-\frac{k_{II}}{\sqrt{2\pi r}} Sin\frac{\theta}{2}\left(2 + Cos\frac{\theta}{2} Cos\frac{3\theta}{2}\right)\right.$$

$$\left. - \upsilon\left(\frac{k_{II}}{\sqrt{2\pi r}} Sin\frac{\theta}{2}\left(Cos\frac{\theta}{2} Cos\frac{3\theta}{2}\right)\right)\right) + \frac{1}{2E}\left(\frac{k_I}{\sqrt{2\pi r}} Cos\frac{\theta}{2}\left(-2 Sin\frac{\theta}{2} Sin\frac{3\theta}{2}\right)\right.$$

$$\left. \frac{-\upsilon k_I}{\sqrt{2\pi r}} Cos\frac{\theta}{2}\left[2 Sin\frac{\theta}{2} Sin\frac{3\theta}{2}\right]\right) + \frac{1}{2E}\left(-\frac{k_{II}}{\sqrt{2\pi r}} Sin\frac{\theta}{2}\left(2 Cos\frac{\theta}{2} Cos\frac{3\theta}{2}\right) -\right.$$

$$\left. \upsilon\left(\frac{k_{II}}{\sqrt{2\pi r}} Sin\frac{\theta}{2}\left(Cos\frac{\theta}{2} Cos\frac{3\theta}{2}\right)\right)\right) Cos\ 2\theta + \frac{1+\upsilon}{E} Sin\ 2\theta\left[\frac{k_I}{\sqrt{2\pi r}} Sin\frac{\theta}{2} Cos\frac{\theta}{2}\right.$$

$$\left. Cos\frac{3\theta}{2} + \frac{k_{II}}{\sqrt{2\pi r}} Cos\frac{\theta}{2}\left(1 - Sin\frac{\theta}{2} Sin\frac{3\theta}{2}\right)\right] \quad (12)$$

Also we could find $\gamma\theta$ as:

$$\frac{1}{2}\gamma\theta = -\left[\frac{1}{2}\left(\varepsilon_x - \varepsilon_y\right) Sin2\theta - \frac{1}{2}\gamma_{xy} Cos\ 2\theta\right]$$

$$= -\frac{1}{2}\left[\frac{1}{2E}\left(\frac{K_I}{\sqrt{2\pi r}} Cos\frac{\theta}{2}\left(-2Sin\frac{\theta}{2} Sin\frac{3\theta}{2}\right) - \upsilon\frac{k_I}{\sqrt{2\pi r}} Cos\frac{\theta}{2}\left[2 Sin\frac{\theta}{2} Sin\frac{3\theta}{2}\right]\right.\right.$$

$$\left.\left.\right) + \frac{1}{2E}\left(-\frac{k_{II}}{\sqrt{2\pi r}} Sin\frac{\theta}{2}\left(2 Cos\frac{\theta}{2} Cos\frac{3\theta}{2}\right) - \upsilon\left(\frac{k_{II}}{\sqrt{2\pi r}} Sin\frac{\theta}{2}\left(Cos\frac{\theta}{2} Cos\frac{3\theta}{2}\right)\right)\right)\right.$$

$$\left. Sin\ 2\theta - \frac{1+\upsilon}{E} Cos\ 2\theta\left[\frac{k_I}{\sqrt{2\pi r}} Sin\frac{\theta}{2} Cos\frac{\theta}{2} Cos\frac{3\theta}{2} + \frac{k_{II}}{\sqrt{2\pi r}} Cos\frac{\theta}{2}\left(1 - Sin\frac{\theta}{2} Sin\frac{3\theta}{2}\right)\right]\right. \quad (13)$$

To find the maximum value of $\varepsilon\theta$, equation (12) is differentiated with respect to θ using math-Lab 2002 program for differentiating, and the derivative is equated to zero. The roots of this equation give values of θ at which max or min of the strain, which are the principal strains in the polar coordinates. The first root is found to be the maximum. The same roots substituted in equation (13) must be given a zero value of shear strain $\gamma\theta$.

These gives two set of equation which relates the ratio $\frac{k_{II}}{k_I}$ and θ for combined effect of mode II and I for crack propagation.

2- It could be related between mixed mode I – II loading involves axial loading in the y direction of a crack inclined as result of rotation a bout the z axis as shown in fig 2-a. Even in this instance, analytical method done by [16] shows that: -

$$KI = (\sigma Sin^2\beta + n\sigma Cos^2\beta)\sqrt{\pi a}$$
$$KII = (\sigma Cos^2\beta + n\sigma Sin^2\beta)\sqrt{\pi a} \quad (14)$$

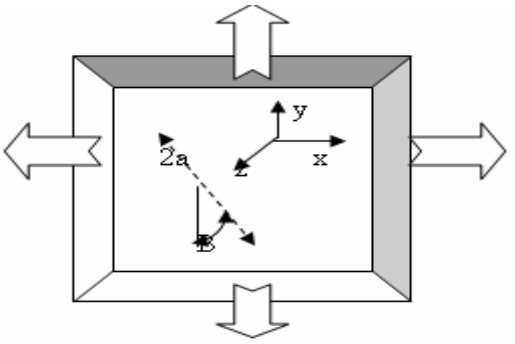

(a)

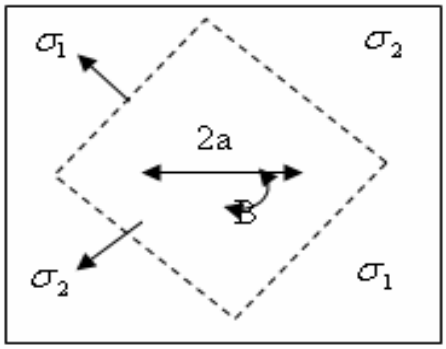

(b)

Figure 2. (a),(b).

Which could be done for very sharp and small crack?

Now by calculating the principle stresses from the condition shown in fig (2-a) and using Mohr's circle construction

$$\sigma_{1,2} = \frac{\sigma_X + \sigma_y}{2} \pm \sqrt{\frac{(\sigma y - \sigma x)^2}{2} + \tau_{xy}^2} \quad (15)$$

Where $\sigma y = 0$ and σx = bending buckling stress
And τ_{xy} = shear buckling stress
By using the values of σ_1, σ_2, the ratio of the stress intensity factories of mode I and II can be calculated from eq (14) as shown in fig (2-b):-

$$KI = (\sigma_1 Sin^2\beta \pm \sigma_2 Cos^2\beta)\sqrt{\pi a}$$
$$KII = (\sigma_1 Cos\beta Sin\beta \pm \sigma_2 Cos\beta Sin\beta)\sqrt{\pi a}\} \quad (16)$$

From group (1) and group (2) of the solution, relation between KII/KI can be obtained for crack propagation and the condition of external loading in which the stress intensity Factor depend on them. The plus minus in eq (16) depend on the value of σ2 as compression or tension.

3):- In this group of solution, we used the fatigue equations of cycling loading by taking the fluctuating of buckling from tension to compression, so that the buckling bending stress will be change its direction, and from Mohers circle the principle stresses may be determined for the maximum and minimum limits of cyclic stresses, by taking the max principal stress in determining the max stress intensity factor as shown by [17] .

$$K_{max} = y(\sigma_{1max} \sin^2 \beta + \sigma_{2max} Cos^2 \beta)\sqrt{\pi a} .....(17 - a)$$

And for min.stress intensity factor

$$K_{min} = y(\sigma_{1min} Sin^2 \beta + \sigma_{2min} Cos^2 \beta)\sqrt{\pi a} .....(17\text{-b})$$

Where y is a correction factor for finite plate and there values depend on the aspect ratio of the plate given in (16).

Knowing that $\sigma_{2\min}$ have mines sign because it is compression, the relation expressing crack growth rates in terms of $\Delta K + Kc$ and a measure of K mean was proposed by [18] in the form:

$$\frac{da}{dN} = \frac{c\Delta k^n}{(1 - R)K_c - \Delta K} \qquad (18)$$

Where c, n=material constants

K_c = fracture toughness

R = load ratio ($\frac{k_{min}}{k_{max}}$)

Δk= kmax - kmin

6. Determination of Stress Intensity Factors

The determination of the mode I and II stress intensity factors was performed by solving eq (12) and eq (16) and is fitted to the mathematical approach of [13] in the form:

$$\frac{K_I}{K_{IC}} + \left(\frac{K_{II}}{k_{IIC}}\right)^2 = 1$$

The determination of the mode I and II stress intensity factors was performed by solving eq (12) and eq (16) and is fitted to the mathematical approach of [13] in the form:

Where

$$K_{IIc} = \sqrt{\frac{2}{3}} k_{Ic}$$

Using a Newton-Raphson iteration scheme, and then it is calculated approximately from the model dimensions and the loads applied.

This work is done for very small crack propagated in the direction of applying buckling load.

7. Results

For the case studies in this research, they taken are from aircraft standard specification duralumin _Bs3L100 Grade 2014 T_4 of rectangular plate with width b=100 mm and thickness t=0.55m for aspect ratio 1,100 mm wide x 100 mm long. And aspect ratios 1.5, 2, 2.5 with crack length 2a=2, 4, 6,8,10 mm under fluctuation of compression and tension buckling stress, where the result gives the effect of this fluctuation on the stress intensity factor (Δk).

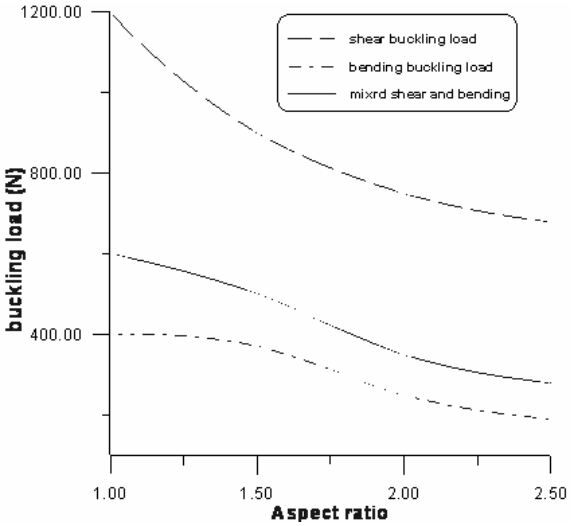

Figure 3. a comparison of theoretical buckling loads for varying boundary conditions.

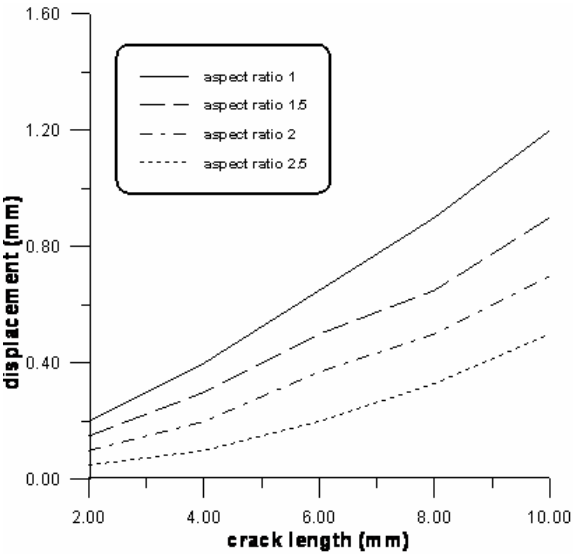

Figure 4.crack length versus u displacement for combined mode I and II from the crack tip.

In fig (3) the theoretical buckling load, for the case of pure shear only and pure bending only, mixed shear and bending stress with different aspect ratios.

It can be shown that shear stress have pronounced effect on the mixed shear and bending, but this effect will be decreased with increasing aspect ratio, so that it become nearer to the bending condition only. The value of bending stress is more pronounced on the crack propagation since in equations (14 , 15 ,and 16). This stress is more effective on the value of KI since they multiplied by $\cos^2\theta$ rather

than KII which multiplied by (sinθ cosθ) for very small values of θ .

From the strain method used in this study, the behavior of the displacement (u) in front of the crack tip with different crack length could be shown in fig(4). The behavior of the displacement will be decreased with increasing aspect ratio, and the rate of decreasing also increased with increasing the crack length. It can be shown also that with increasing the crack length for the same aspect ratio, the displacement will be increased, but the rate of increasing in the displacement are decreased with increasing aspect ratio.

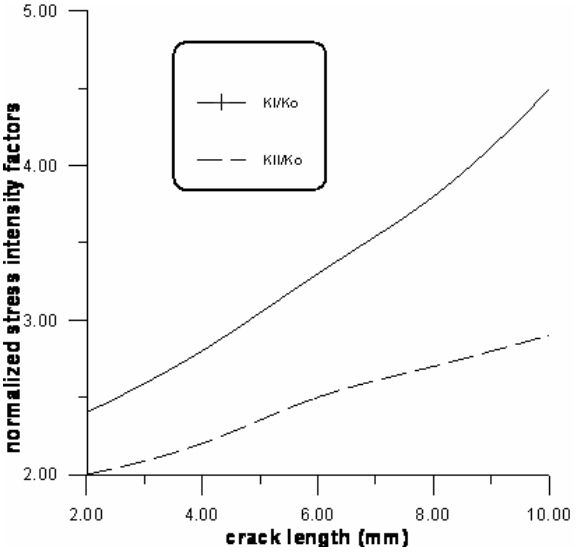

figure 5. Normailized Stress intensity factors as a function of crack length for aspect ratio 1.

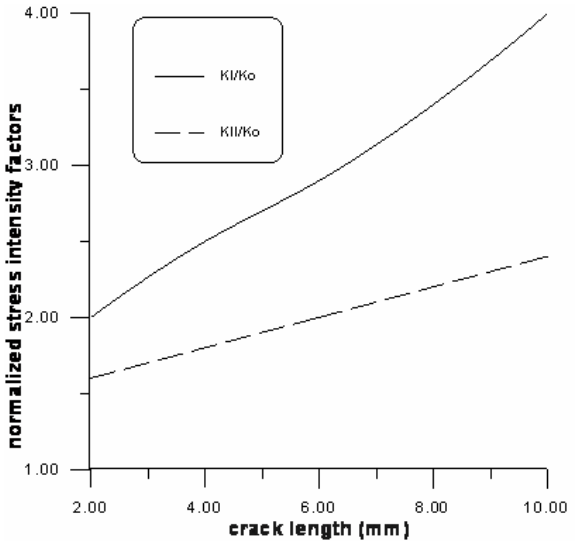

figure 6.normalized stress intensity factors as a function of crack length for aspect ratio 1.5.

In figures (5),(6),(7) , and (8), the data obtained from this process were the normalized stress intensity factors K1/K0 and KII/K0 , where K0 = $\sigma_0\sqrt{\pi a}$ and σ_0 is the applied or normal stress. For different crack length, the values of KI/K0 and KII/K0 will be increased with increasing crack length, but these values decreased with increasing aspect ratio. It is worthntoing that the values of KII have small values for aspect ratio of 2.5 which means

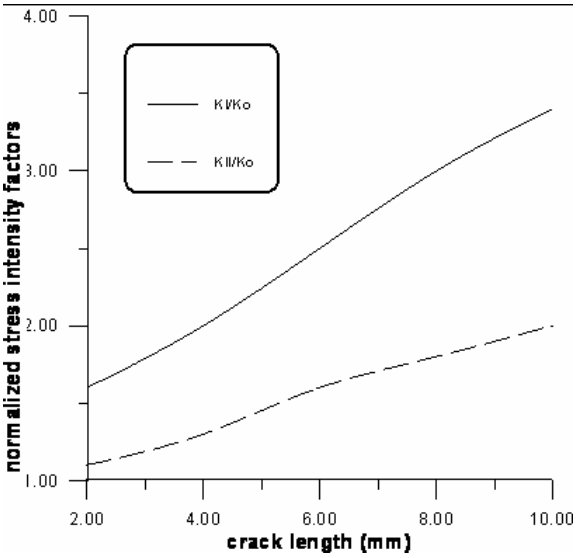

figure 7.normalized stress intensity factors as a function of crack length for aspect ratio 2.

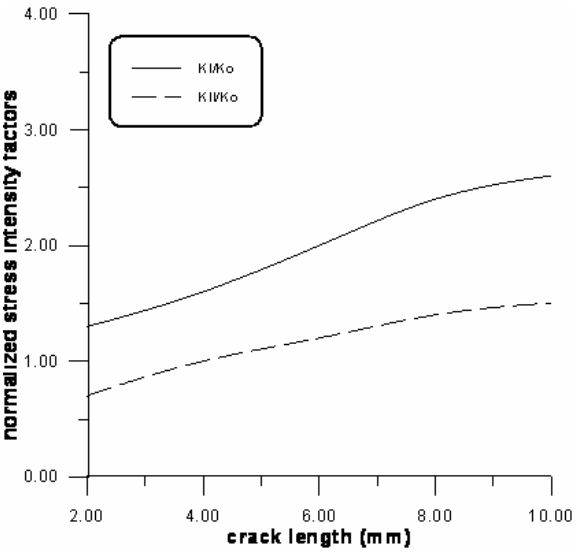

figure 8.normalized stress intensity factors as a function of crack length for aspect ratio 2.

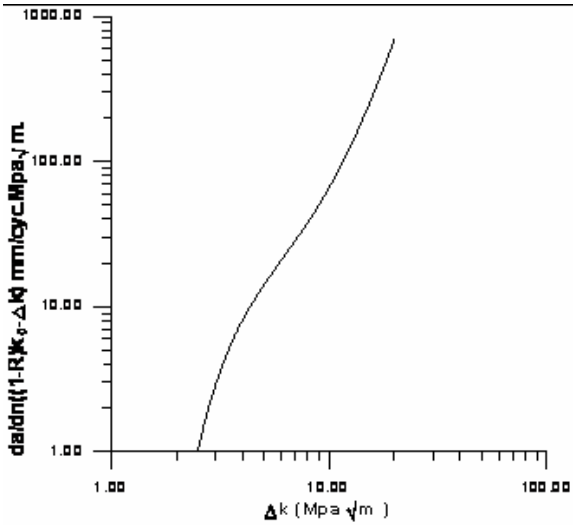

figure 9.fatigue crack propagation in aliminum plate with (2a=2mm) showing the effect of Δk vs.da/dn.

that the mode I fracture is more effective than mode II fracture with increasing aspect ratio of the thin plate. The

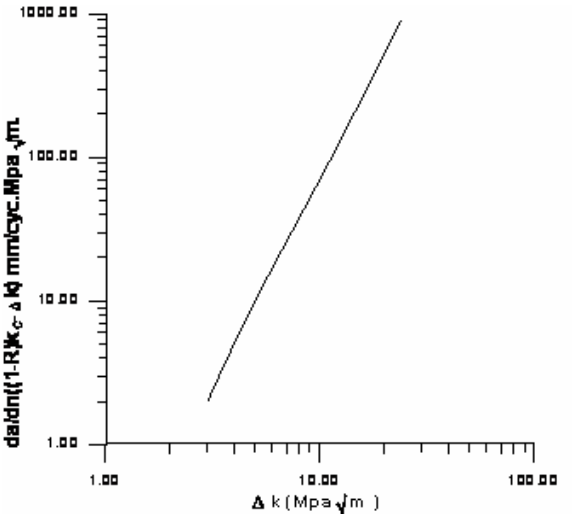

figure 10.fatigue crack propagation in aliminum plate with (2a=4mm) showing the effect of Δk vs.da/dn.

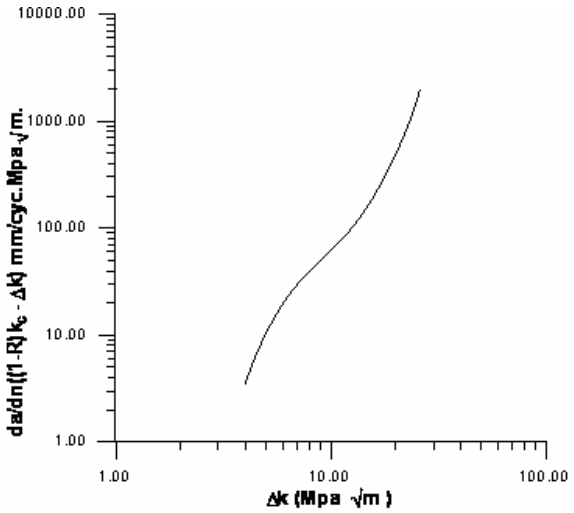

figure 11.fatigue crack propagation in aliminum plate with (2a=8mm) showing the effect of Δk vs.da/dn.

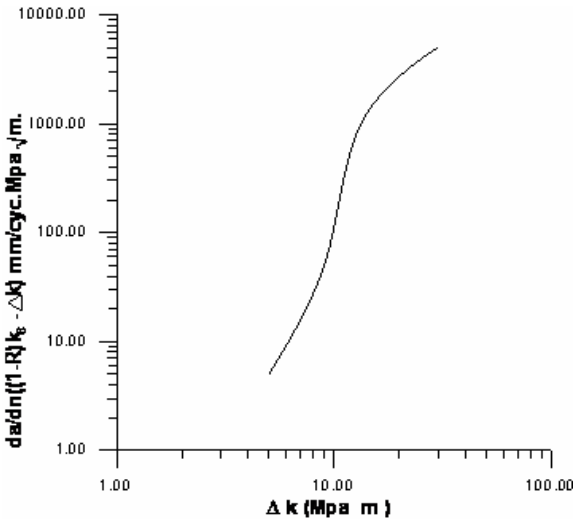

figure 12.fatigue crack propagation in aliminum plate with (2a=8mm) showing the effect of Δk vs.da/dn.

results show that the variation in the values of KI and KII depends not only on the values of the normal and shear stresses, but also on other factors like aspect ratio, and the

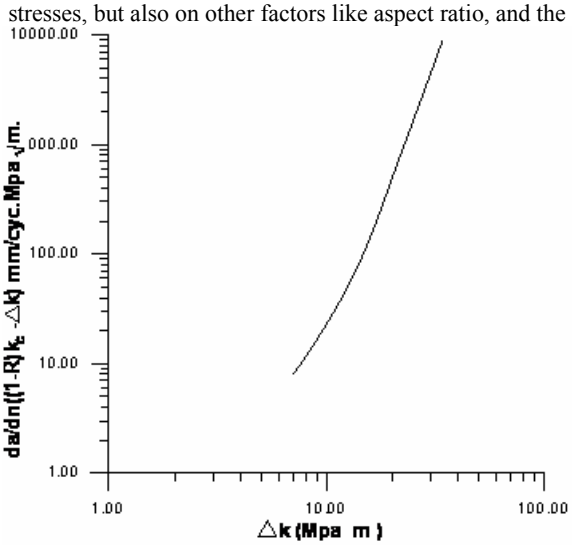

figure 13.fatigue crack propagation in aliminum plate with (2a=10mm) showing the effect of Δk vs.da/dn.

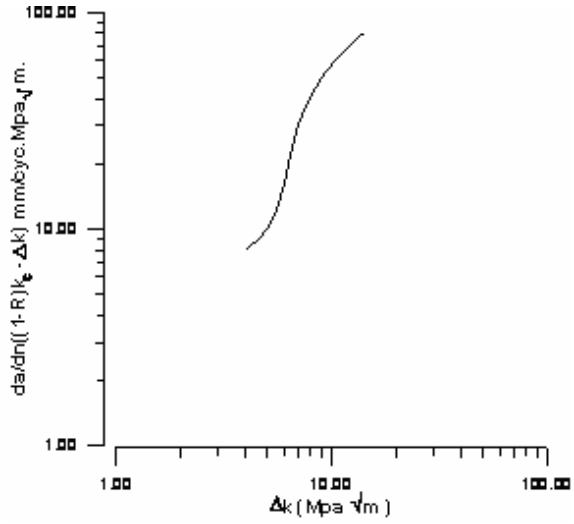

(a)

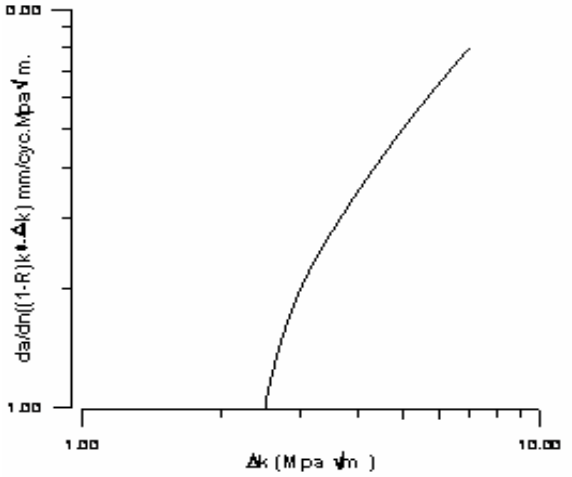

(b)

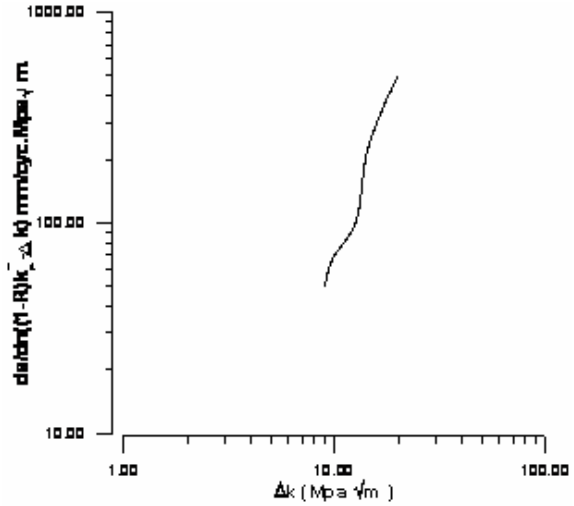

(c)

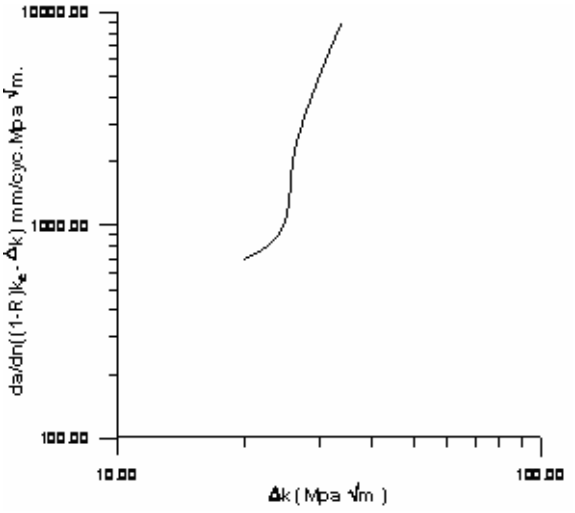

(d)

Figure 14. (a) fatigue crack in aluminum plate with aspect ratio = 1 showing the effect of Δk vs.da/dn, (b) fatigue crack in aluminum plate with aspect ratio = 1.5 showing the effect of Δk vs.da/dn, (c) fatigue crack in aluminum plate with aspect ratio = 2 showing the effect of Δk vs.da/dn, (d) fatigue crack in aluminum plate with aspect ratio = 2.5 showing the effect of Δk vs.da/dn.

ratio of crack length to the aspect ratio which is shown in these figures.

Calculating the fatigue crack propagation, by using Forman equation in four cases of aspect ratios (1, 1.5, 2, 2.5) which results in four points connected by spline fitting, gives good observation about the relation between Δk versus da/dN for cycling buckling loads for thin plates, figures (9 , 10 and 11) .

It can be seen the effect of increasing the crack length causes increasing in the value of Δk and increasing in the Forman cycling load

$$\left(\frac{da}{dN}\right)\left[(1-R)K_c - \Delta K\right] \text{mm / cyc.Mpa } \sqrt{\text{m.}}$$

It can be seen that increasing the aspect ratio causes an increase in the $\frac{da}{dN}$ but the rate of increasing will be decreased when we transfer from aspect ratio 2 to 2.5, and this is because the effect of stress ratio will be more effective than the change in Δk on the value of da/dN. Also from figures (12) and (13) increase the crack length and increasing the aspect ratio to values 2 and 2.5 cause very high values of da/dN which are corresponding to the effect of increasing of mode I (KI) and decreasing in the mode II (KII) in these boundary condition.

It could bee shown from figures (14-a, b, c, d) that the variation of aspect ratio for crack lengths (2a=2,4,6,8,10 mm) causes nonlinearity in the behavior of Δk versus (da/dn [(1-R) kc-Δk] mm/cyc.MPa √m, and the rate of increasing will not be changed uniformly because the effect of combined mode I and II and the complexity of the fluctuating of buckling loads and its effect on the fatigue crack growth for high aspect ratio.

8. Conclusions

It has been shown that the method developed for redistricting crack paths using combined maximum principle strain and maximum principle stress give good results when compared with experimental results that have been obtained previously by some researchers for thin plate with small crack initiation [19]. Then this method has been used for predicting the crack growth for many aspect ratio and its effect on the values of cycling loading da/dN. The results show that increasing aspect ratio and crack length causes very high values of da/dN and assist that the crack propagate under mode I rather than mode II. Also in this research it takes into consideration the variation of Δk with different aspect ratios for the same applied fluctuating stresses.

References

[1] W. Ritz, “jairnal fur reine und angewandte Mathematic”. Vol. 135(1), 1909, 1-61.

[2] Young W C. Roarks formulas for stress and strain. London: McGraw-Hill; 1989.

[3] Timoshenko S P, Gere J M. Theory of elastic instability. London: McGraw- Hill; 1961.

[4] Bruhm E F. Analysis and design of flight vehicle structures. Indianapolis: Jacobs publishing Inc.; 1973 .

[5] C.A. Feathereston, C. Ruiz, “Buckling of flat plates under bending and shear”. Journal of Mechanical Engineering science, Vol. 212, 1998, 249-261.

[6] A.D.Nurse, E.A.Patterson” Determination of predominantly mode it stress intensity factors from isochromatic data”. Fatigue and fracture of Engng Mater. Structure, 16(12), 1993,1339-1354

[7] D.R.Tadjive , S.T.Ki ,”fatigue crack growth prediction in 7475-T7351 Aluminum Alloy under Random loading using modified root mean square model “, Yeungnam university , South Korea , 2003,712-749 .

[8] R. Doglione , M. Bartolone, “Fatigue crack propagation in 2195-T8 Aluminum alloy plate”. 9th International conference on Aluminium Alloys (ICAA9) , Institute of materials Engineering Australasia , 2004, 616-621 .

[9] Y. Liu, S. Mahadevan ,” Threshold stress intensity factor and crack growth rate prediction under mixed – mode loading”. Engineering Fracture Mechanics , Vol. 74 , 2006, 332-345 .

[10] P.J. Forsyth, “A two stage process of fatigue crack growth”. In proceedings of the crack propagation symposin, canfield, Bedfordshire, 1961, 76-94.

[11] A.H. Cottrell, “Theoretical aspects of radiation damage and brittle fracture in steel pressure vessels”. Iron Steel Institute, Special Report No.69 , 1961, 281-296.

[12] S.K. Maiti, R.A.Smith, "Criteria of brittle fracture in biaxial tension". Engineering Fracture Mechanics , Vol. 19, No.5, 1984,739-804 .
[13] Hellan K. Introduction to fracture mechanics. London: Mc Graw –Hill; 1985.
[14] Batdorf S B. A simplified method of elastic stability analysis for thin cylindrical shells I- Donnells equation. NACA TN 1341; 1947.
[15] I.T. Cook, K.C. Rockey, "Shear buckling of rectangular plates with mixed boundary conditions". Aeronauta , 14 ,1963 .
[16] P.C.Paris., G.C.sih ,. ASTM STP 381, 1965, 30.
[17] Hertzbeg W R. Deformation and fracture mechanics of Engineering materials. John Wiley and Sons; 1996.
[18] [18] R.G. Forman, V.E. Kearrey,R.M.Engle, J.Basic Engineering Trans .ASME89459 , 1967.
[19] Ewalds H L, Wanhilll R J. Fracture mechanics. Edward Arnold publication; 1989.
[20] ASTM standard E647-93. 1993 Annual Book of ASTM Standards. Philadelphia, PA; 1993.
[21] R.I. Burguete, E.A.Patterson,"The effect of friction on crack propagation in the dovetail fixings of compressed discs". J. Mechanical Eng. Science, Vol. 212, Part c, 1998, 171 .